Electronic Supplementary Material (ESI) for Journal of Materials Chemistry B.

Supplemental Material

Carbon dots with red emission as a fluorescent and colorimeteric dual-readout probe for the detection of chromium(VI) and cysteine and its logic gate operation

Yifang Gao,[a] Yuan Jiao,[a] Wenjing Lu [a] Yuanyuan Ding, [a] Hui Han, [a] Xiaojuan Gong,[a]
Ming Xian,[a, b] Shaomin Shuang [a] and Chuan Dong*[a]

[a]*Institute of Environmental Science, and School of Chemistry and Chemical Engineering, Shanxi University, Taiyuan 030006, China*
[b]*Department of Chemistry, Washington State University, Pullman, WA, 99164, USA*

*Corresponding author. Tel: +86-351-7018613; fax: +86-351-7018613.
E-mail addresses: dc@sxu.edu.cn (C. Dong).

Experimental

Instrumentations

Transmission electron microscope (TEM) images were obtained on a JEOL JEM-2100 transmission electron microscope (Tokyo, Japan) at a voltage of 300 kV. Absorption spectra were collected using a Lambda 365 spectrophotometer (PerkinElmer, Llantrisant, U.K.). Fluorescence spectra and steady-state fluorescence were recorded on a Hitachi F-4500 fluorescence spectrophotometer. Absorption spectra were recorded using a Lambda 365 spectrophotometer (PerkinElmer, Llantrisant, U.K.). X-ray photoelectron spectroscopy (XPS) data was gotten using an AlKα radiation at 1486.6 eV on an AXIS ULTRA DLD X-ray photoelectron spectrometer (Kratos, Tokyo, Japan).Elemental analysis data were achieved by analysis of elemental analysis system element EL cube element analyzer (Hanau, Germany). Spectral plots were fitted to the peak fitting program via a symmetric symmetrical Gaussian-Lorentzian function through Case XPS v.2.3.12 software. A Fourier transform infrared (FTIR) spectra was tested on a Bruker Tensor ΠFTIR spectrometer (Bremen, Germany). The time-resolved luminescence spectra were measured by means of the Edinburgh FLS920 fluorescence spectrophotometer. Images were accomplished through a confocal laser scanning microscope (LSM880+Airyscan, Zeiss).

Determination of QY

Quantum yields(QY)of the CDs was concluded by a widely accepted relative method.[24] Specifically, rhodamine 6B (QY =56% in ethanol) was voted as the reference. The QY of a sample was determined by the following equation:

$$\phi_S = \phi_R(Grad_S/Grad_R)\ (\eta^2_S/\eta^2_R)$$

where Grad is the gradient from the plot of integrated fluorescence intensity against absorbance and η(1.36) is the refractive index of the solvent. The subscripts S and R represent CDs and the reference (rhodamine 6B in ethanol). To prevent the re-absorption effect, the absorbances of CDs and rhodamine 6B solutions in the 10mm fluorescence cuvette were adjusted to less than 0.10 at the excitation wavelength (λex) of 524 nm (i.e., the absorption maximum of CDs). The integrated fluorescence intensity was the area under the PL curve in the wavelength range 540-750 nm.

Table S1. Elemental analysis of the as-synthesised CDs.

Sample name	Elemental content (%)				
	C	H	N	P	O (Calculated)
CDs	26.6	4.7	1.2	15.6	51.9

Table S2. Lifetime calculations from the time-resolved decay profiles of CDs and CDs@Cr(VI).

Sample	τ1 (ns)	Percentage (%)	τ2 (ns)	Percentage (%)	Ave.τ (ns)
CDs	1.6984	71.44	1.7260	72.32	3.771
CDs@Cr(VI)	8.9574	28.56	8.8650	27.68	3.701

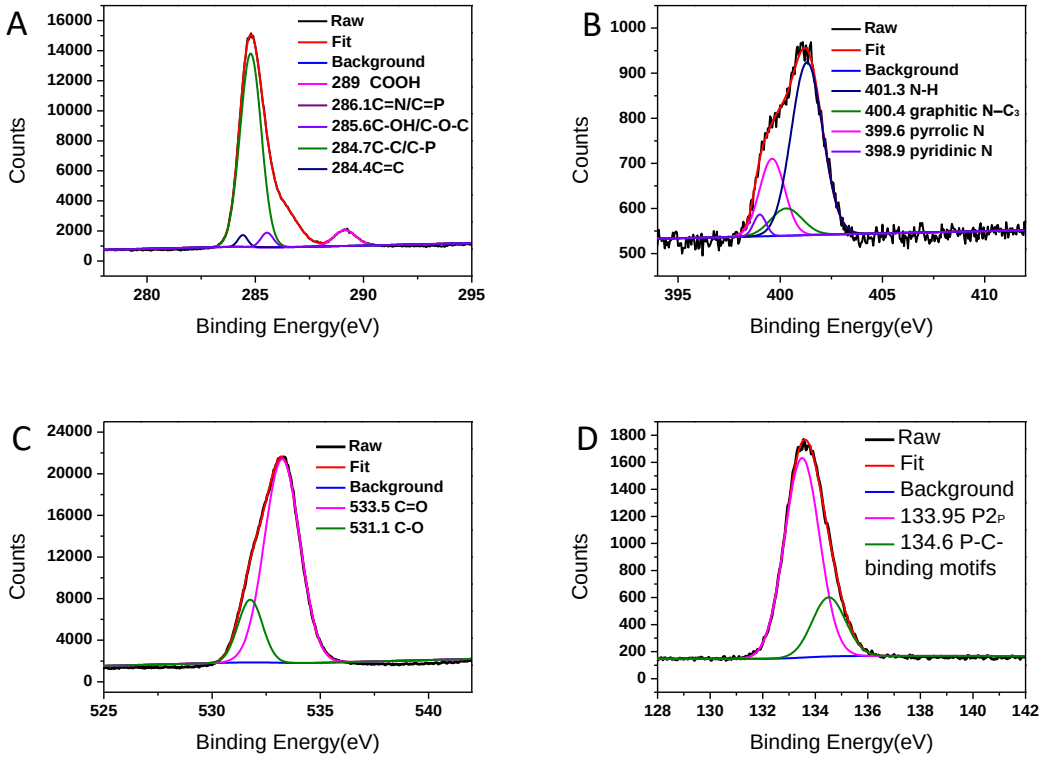

Fig. S1 High-resolution XPS data of C 1s (A), N 1s (B) , O1s (C) and P2p (D) of CDs.

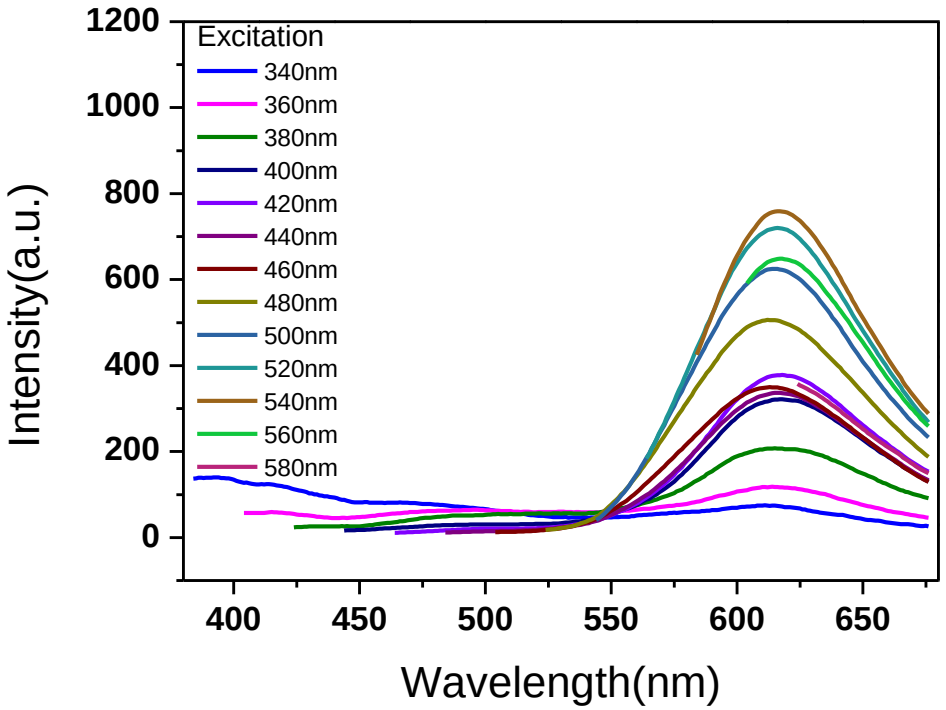

Fig. S2 FL emission spectra of the CDs under different excitation wavelengths.

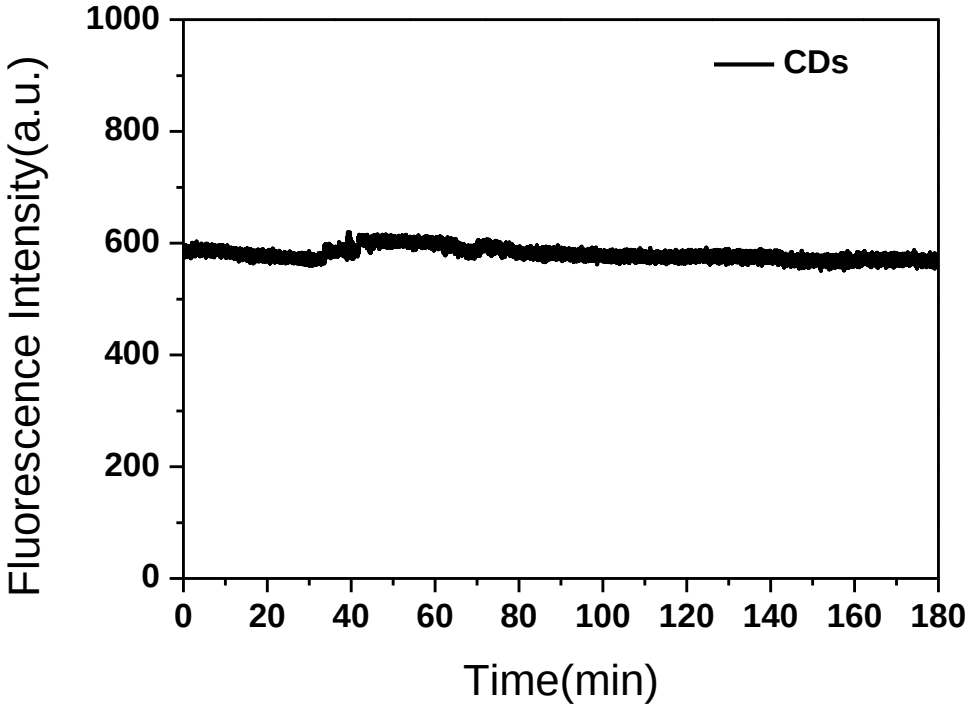

Fig. S3 Effect of time intervals of irradiation with xenon arc light on FL intensity of CDs.

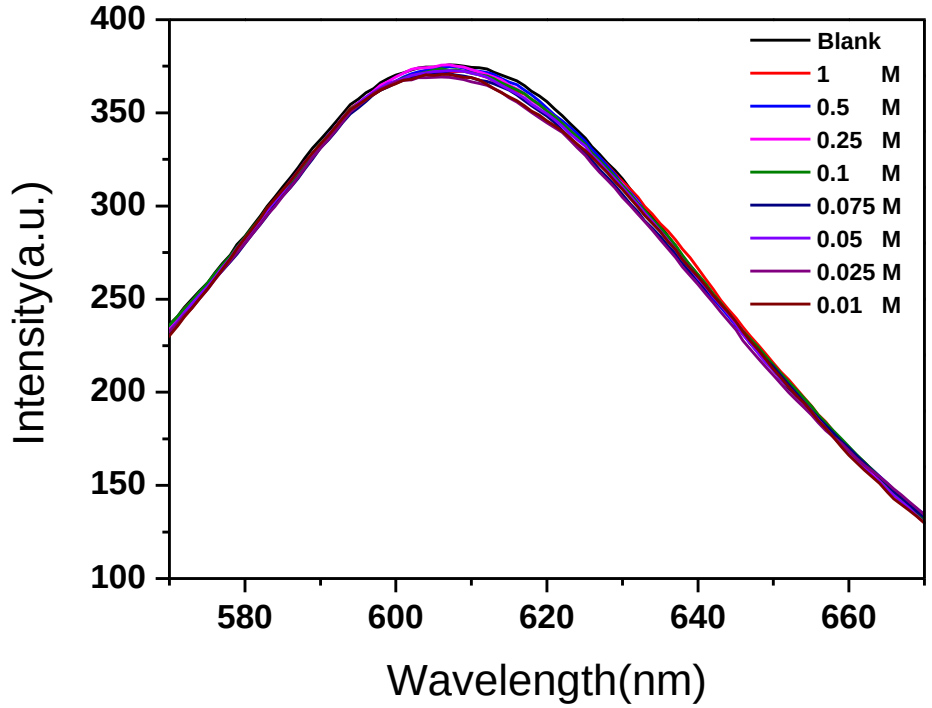

Fig. S4 Effect of ionic strength on fluorescence intensity of CDs.

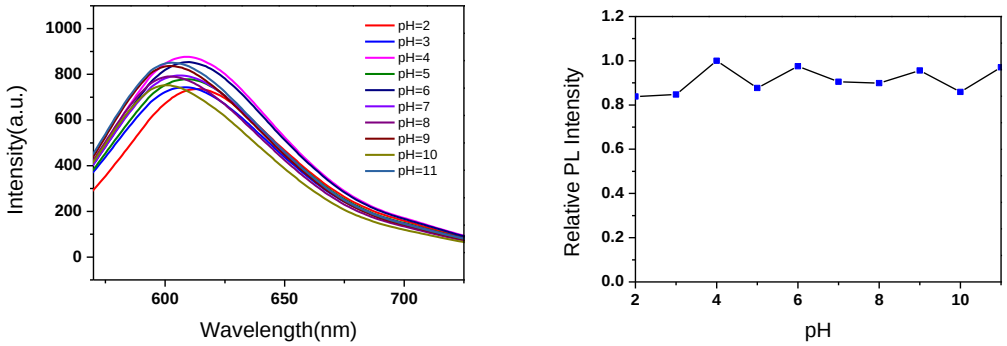

Fig. S5 (A) The fluorescence emission spectra of the CDs under different pH values. (B) The normalized fluorescence emission spectra of CDs (25 μg·mL) at 617 nm at different pH values.

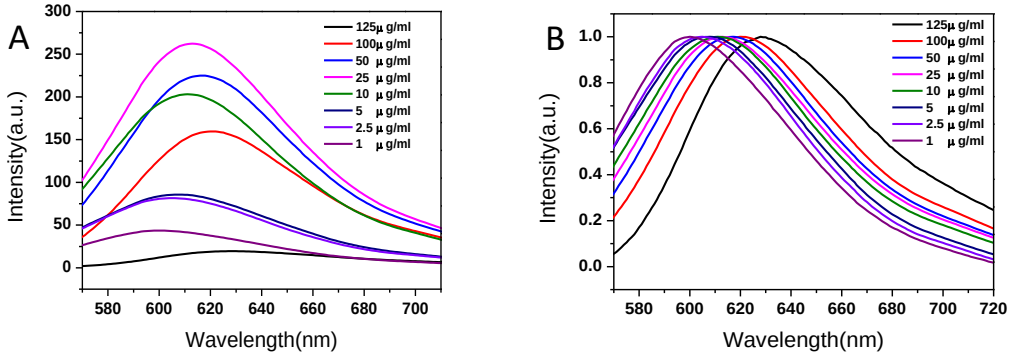

Fig. S6 (A) The fluorescence emission spectra of the CDs aqueous solutions with different concentrations. (B) The normalized fluorescence emission spectra of CDs aqueous solutions with different concentrations.

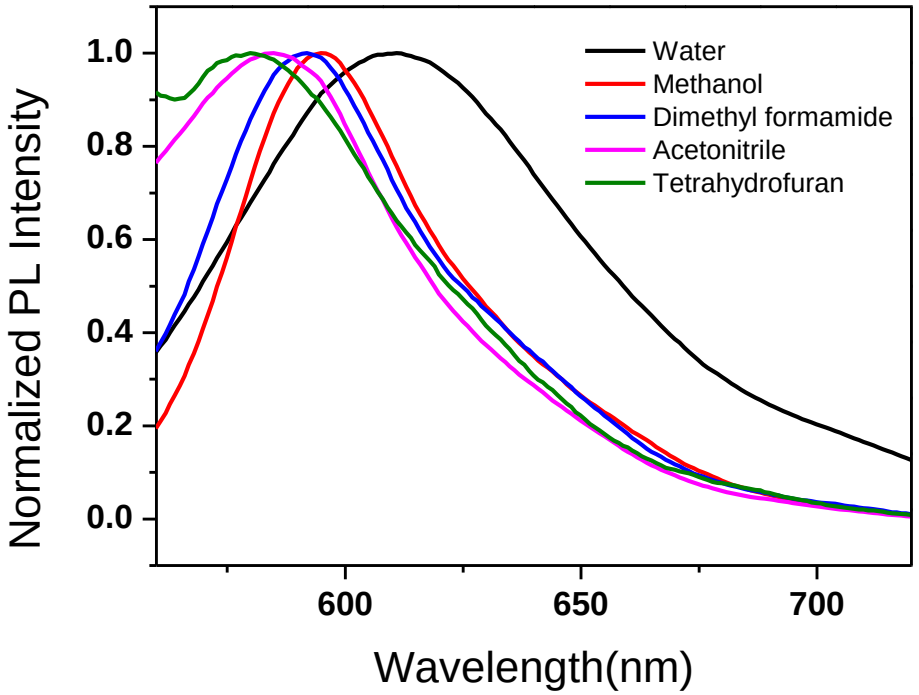

Fig. S7 The normalized fluorescence emission spectra of CDs (25 μg·mL^{-1}) in different solvents.

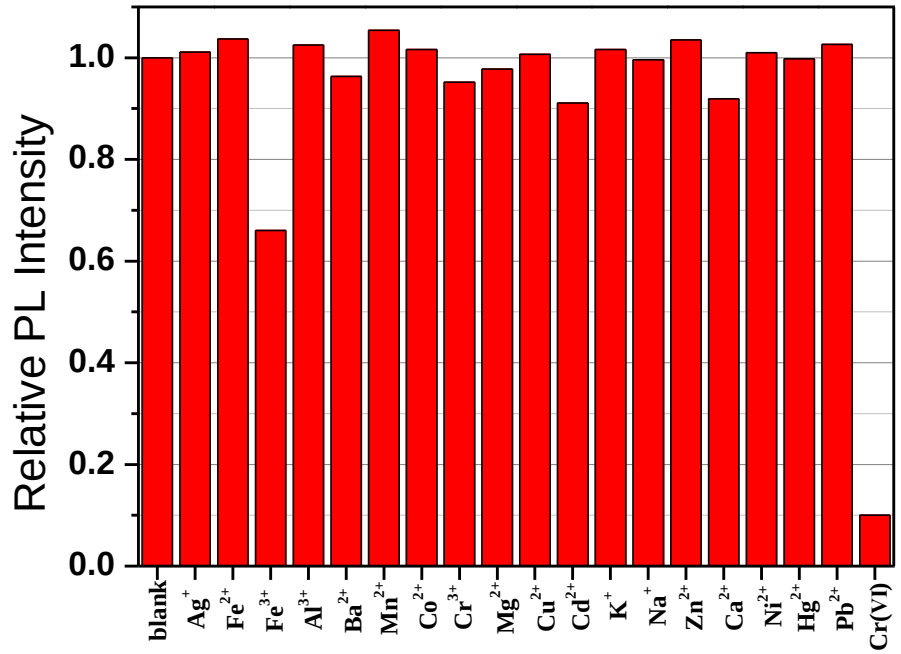

Fig. S8 The influence of different metal ions on the fluorescence of CDs.

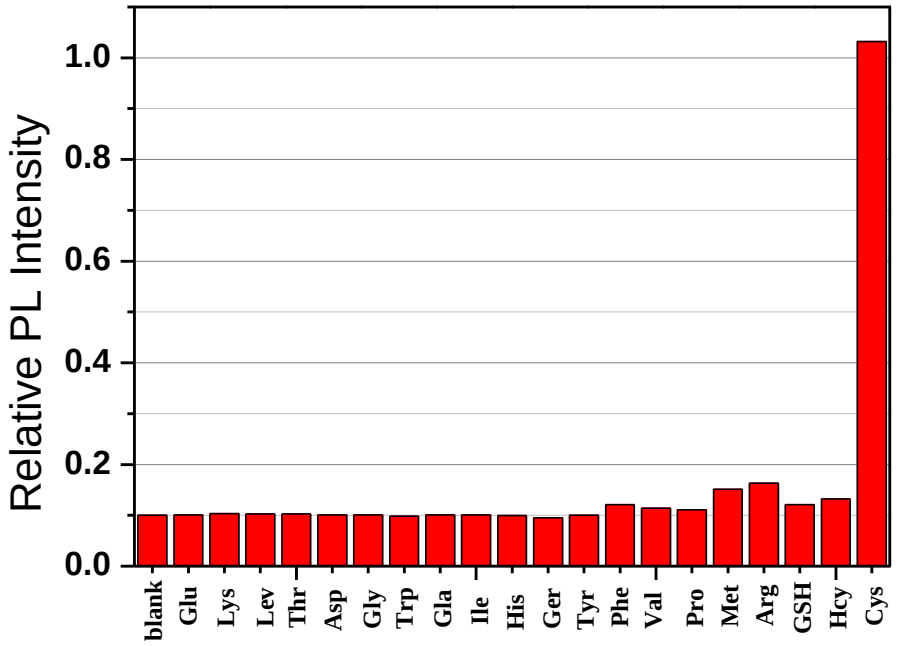

Fig. S9 The influence of different different amino acids on the fluorescence of CDs@Cr(Ⅵ), the he blank is representative of CDs@Cr(VI).

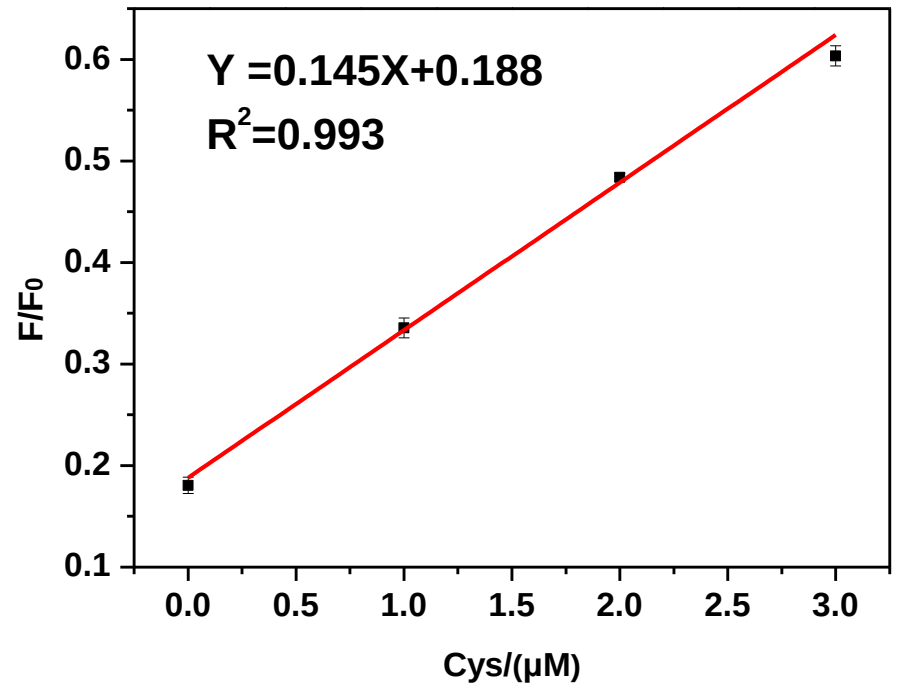

Fig. S10 Plot of the absolute change of the FL intensity of CDs@Cr(Ⅵ) versus the concentration of Cys.

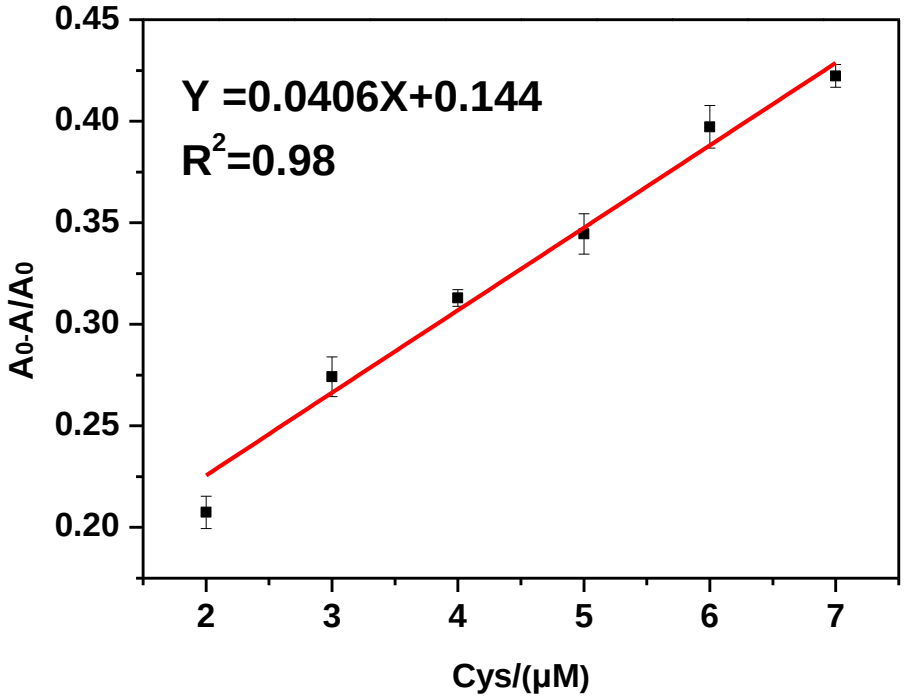

Fig. S11 Plot of the absolute change of the absorption intensity of CDs@Cr(Ⅵ) versus the concentration of Cys.

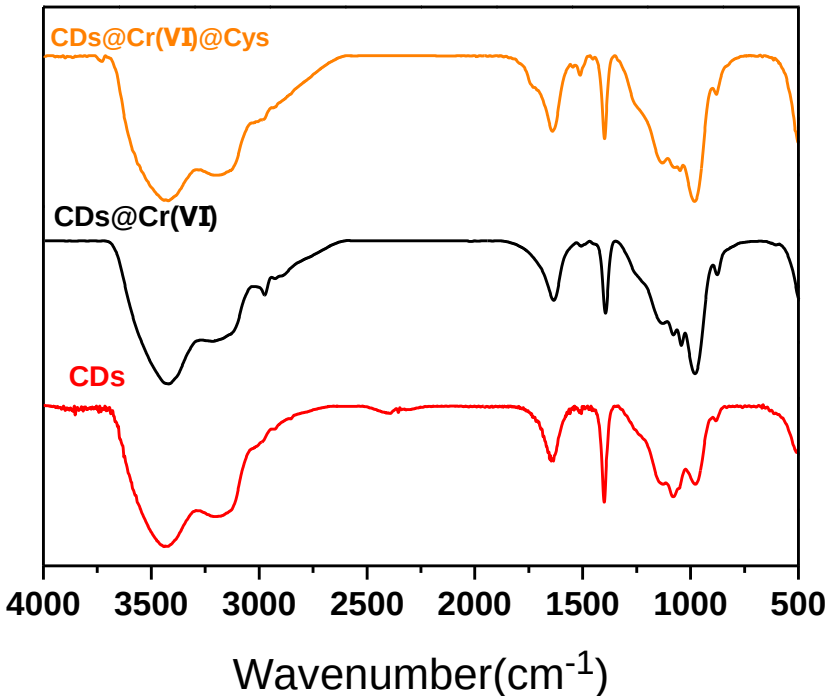

Fig. S13 The FT-IR spectrum of the CDs, CDs@Cr(Ⅵ) and CDs@Cr(Ⅵ)@Cys.

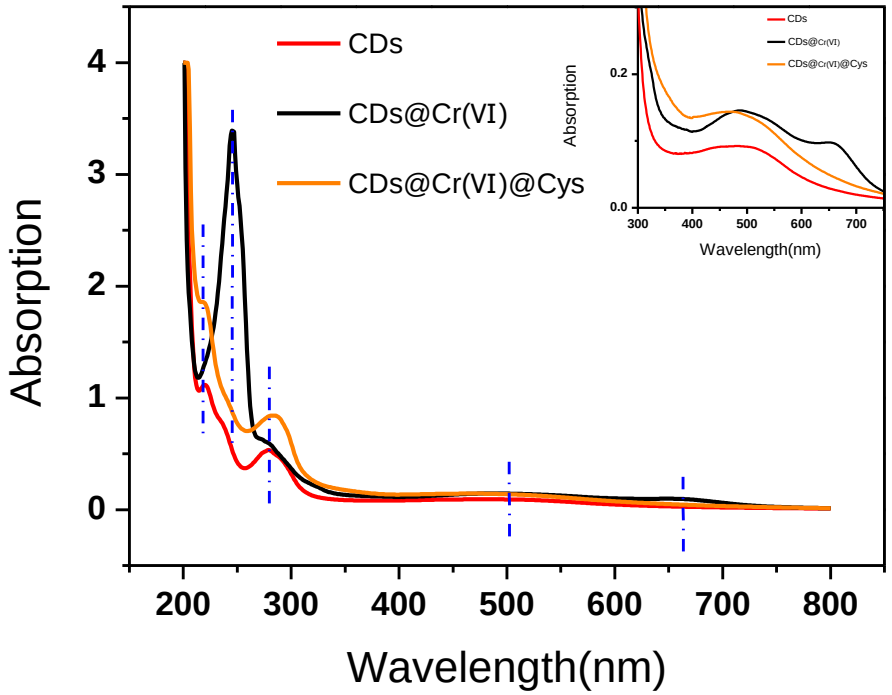

Fig. S14 The UV-vis spectra of the CDs, CDs@Cr(Ⅵ) and CDs@Cr(Ⅵ)@Cys in aqueous solution.

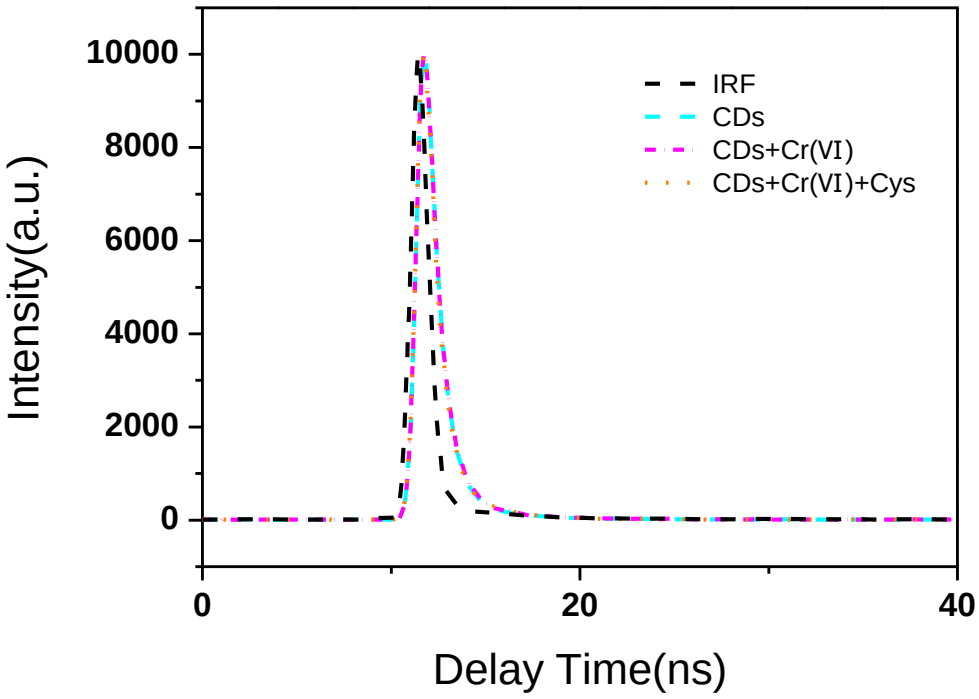

Fig. S15 The fluorescence emission decay curves of CDs, CDs@Cr(Ⅵ) and CDs@Cr(Ⅵ)@Cys in aqueous solution.

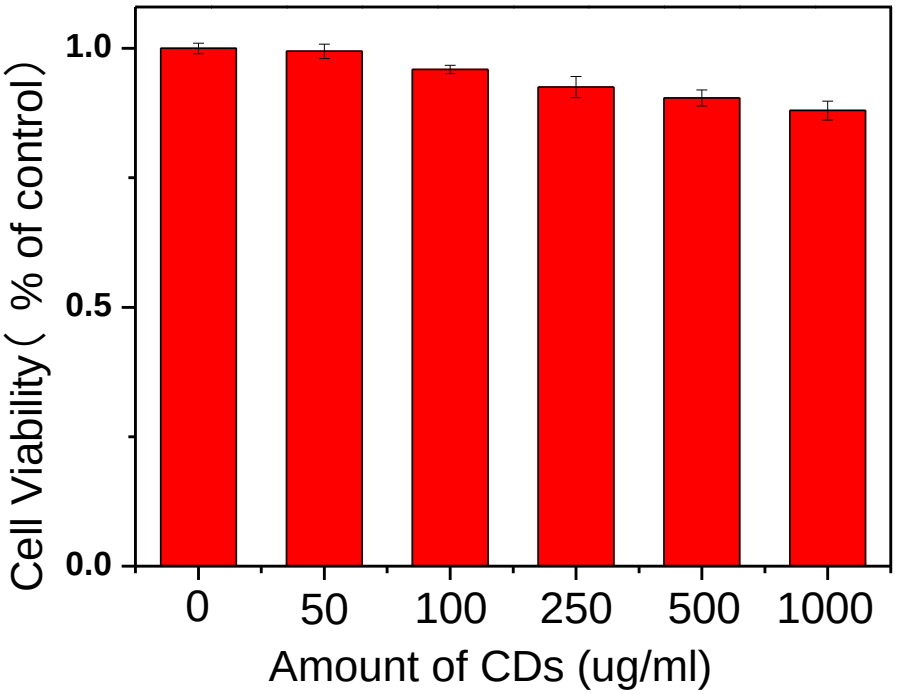

Fig. S17 Cytotoxicity testing results of CDs on SMMC7721cells viability. The values represent percentage cell viability (mean% ± SD, n=6).

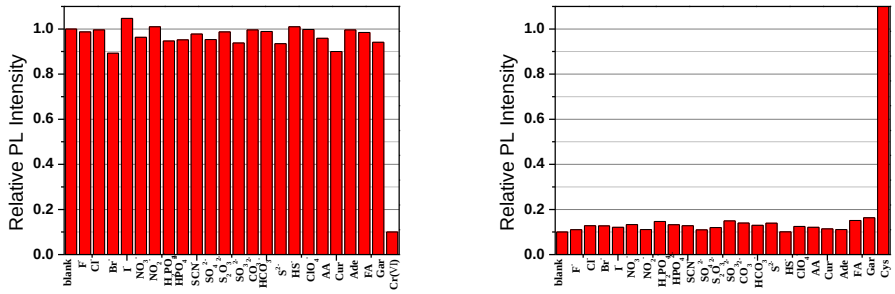

Fig. S18 The influence of different various anions and some biomolecules on the fluorescence of CDs (A), CDs@Cr(Ⅵ) (B), respectively. The he blank is representative of CDs , CDs@Cr(VI), respectively.

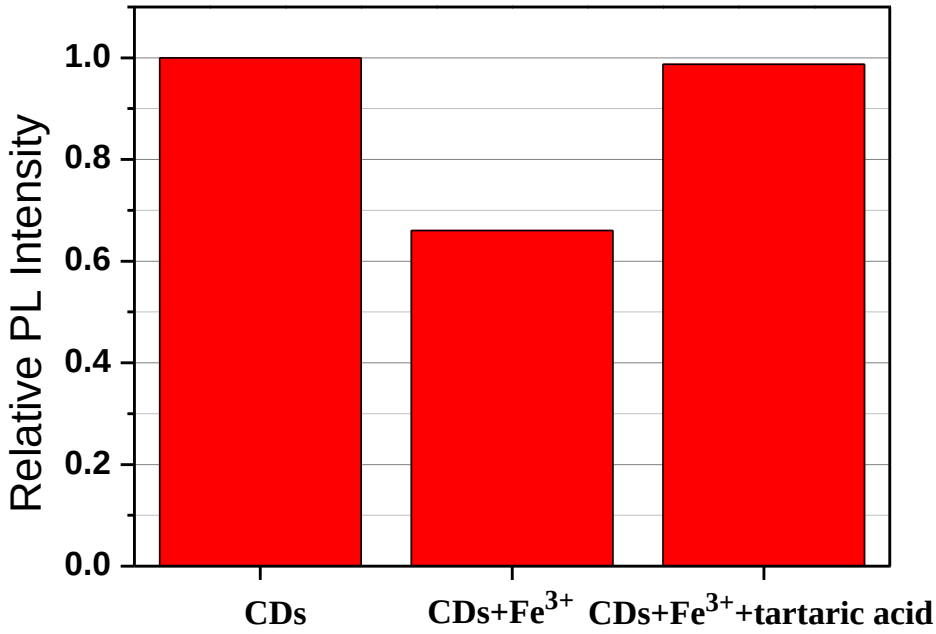

Fig. S19 FL intensity of CDs, CDs+Fe^{3+} and CDs+Fe^{3+}+ tartaric acid with the addition of Fe^{3+} (0.5 mM) and tartaric acid (1 mM, masking agent), respectively.